ORIGINAL ARTICLE

WILEY

Evaluation of chicken chorioallantoic membrane model for tumor imaging and drug development: Promising findings

Lizhen Wang[1,2] | Junjie Yan[2] | XinyuWang[2] | Yuping Xu[2] | Donghui Pan[2] |
Chongyang Chen[2] | Ying Shao[1] | Xiangjun Song[1] | Kezong Qi[1] | Min Yang[2] |
Jian Tu[1] [ORCID]

[1]Anhui Province Engineering Laboratory
for Animal Food Quality and Bio-safety,
College of Animal Science and Technology,
Anhui Agricultural University, Hefei, China

[2]NHC Key Laboratory of Nuclear
Medicine, Jiangsu Key Laboratory of
Molecular Nuclear Medicine, Jiangsu
Institute of Nuclear Medicine, Wuxi, China

Correspondence
Min Yang, NHC Key Laboratory of Nuclear
Medicine, Jiangsu Key Laboratory of
Molecular Nuclear Medicine, Jiangsu
Institute of Nuclear Medicine, Wuxi,
Jiangsu 214063, China.
Email: yangmin@jsinm.org

Jian Tu, Anhui Province Engineering
Laboratory for Animal Food Quality and
Bio-safety, College of Animal Science and
Technology, Anhui Agricultural University,
Hefei 230036, China.
Email: tj-0531@ahau.edu.cn

Abstract

Background: The chicken chorioallantoic membrane (CAM) model is a potential alternative to the mouse model based on the 3R principles. However, its value for determination of the in vivo behaviors of radiolabeled peptides through positron emission tomography (PET) imaging needed investigation. Herein, the chicken CAM tumor models were established, and their feasibility was evaluated for evaluating the imaging properties of radiolabeled peptides using a ^{68}Ga-labeled HER2 affibody.

Methods: Two human breast cancer cell lines were inoculated into chicken CAM and mice, respectively. The tumor-targeting potential and pharmacokinetic profile of a ^{68}Ga-labeled affibody, ^{68}Ga-MZHER, in both tumor models were also determined.

Results: The tumor-formation time in chicken CAM model was shorter than that of mouse model. The uptake values of human epithelial growth factor receptor-2 (HER2)-positive Bcap37 tumors in chicken CAM and mouse models were $5.36 \pm 0.26\%$ ID/g and $5.26 \pm 0.43\%$ ID/g at 30 min postinjection of ^{68}Ga-MZHER, respectively. At the same time points, the uptake values of HER2-negative MDA-MB-231 tumors in the chicken CAM models and mouse models were $1.57 \pm 0.15\%$ ID/g and $1.67 \pm 0.25\%$ ID/g, respectively. Ex vivo biodistribution confirmed that more radioactivity accumulated in Bcap37 tumors than in MDA-MD-231 tumors in both CAM and mouse models.

Conclusion: In this study, the CAM tumor model was successfully prepared. The chicken CAM model is a novel tool for quickly determining the in vivo properties of radiolabeled peptides targeting biomarkers. It may be beneficial for early monitoring of the therapeutic effect of a new drug through PET imaging with specific peptides.

KEYWORDS
^{68}Ga, affibody, chicken embryo CAM, HER2, PET imaging

1 | INTRODUCTION

Human epithelial growth factor receptor-2 (HER2) is a transmembrane receptor-like protein and is involved in cell growth, activation, and proliferation by activating the downstream signaling pathway.[1] HER2 is lowly expressed in normal tissues but is overexpressed in malignant tumors, such as breast cancer and gastric cancer.[2-4] Tumors with abundant HER2 levels were found to be more aggressive and tend to spread faster than HER2-negative tumors. The survival of HER2-positive tumors was also poorer. Therefore, HER2 is an important biomarker for tumor theranostics. Precise assessment of HER2 status in tumors is the cornerstone of accurate diagnosis and therapy.[5]

Biopsy is a commonly used method to determine the HER2 levels in clinical settings. However, limited by the heterogeneity, the sample may not reflect the whole tumor characteristics. Compared with biopsy, non-invasive positron emission tomography (PET) provides an effective and reliable technology for the whole body detecting HER2 levels, with the advantages of higher sensitivity and real-time and quantitative analysis.[6,7]

Specific tracers targeting HER2 are the basis for carrying out accurate HER2 PET imaging. Affibody is a small-sized protein consisting of dozens of amino acid residues. It is a favorable ligand targeting HER2 with the advantages of high-affinity convenient synthesis, fast blood clearance, rapid concentration in target tissues, and no immunogenicity.[8-10] Previous studies confirmed that a 68Ga-labeled HER2 affibody, 68Ga-MZHER, is an ideal probe for detecting the HER2 levels in tumors. It exhibits satisfactory image properties and may play specific roles in disease management and development of new drugs.[11-13]

Traditionally, mice-bearing transplantation tumors were established for preclinical evaluation of the pharmacokinetics or pharmacodynamics of agents targeting tumors. However, the cost to feed the murine models in the animal facility is high, and the application of animals in research was regulated concerning the welfare of the laboratory animals. The chicken embryo chorioallantoic membrane (CAM) is a low-cost, reproducible, and reliable alternative model to investigate the functional features of tumor biology, such as growth, angiogenesis, and metastasis.[14,15] Due to the highly vascularized extraembryonic membrane, the chicken CAM could provide abundant nutrient cultures, such as a rich vascular network, for the spontaneous growth of human tumor cells.[16,17] Moreover, the chicken CAM is a naturally immunodeficient host enabling the formation of xenograft tumors. Thus, CAM models may be an ideal platform for evaluating the performance of pharmacological compounds, including radiopharmaceuticals.

In this study, a CAM model implanted with tumors was established, and its feasibility for monitoring HER2 levels through PET imaging with the 68Ga-labeled HER2 affibody was also determined (Figure 1).

2 | MATERIALS AND METHODS

2.1 | Ethics statement

This study was approved by the Ethics Committee of Jiangsu Institute of Nuclear Medicine and complies with the institutional guidelines (no: 2022-JSINM-077).

2.2 | Materials

Anti-Ki67 antibody and anti-ErbB2/HER2 antibody were purchased from Abcam. The DAB staining solution (polymeric method) secondary antibody kit was purchased from Genentech. Anti-β-actin and HRP monoclonal goat anti-rat/rabbit immunoglobulin G (IgG) were purchased from Shanghai Biyuntian Biotechnology Co., Ltd. Donkey anti-rabbit secondary antibodies and donkey anti-mouse secondary antibodies were purchased from Thermofisher. Other reagents were purchased from Sinopharm Chemical Reagent Co., Ltd. 68Ga-MZHER was synthesized based on the previous literature, and the radiopurity was greater than 95%.[13]

2.3 | Cells and animals

Bcap37 human breast cancer cells and MDA-MB-231 human breast cancer cells were purchased from Shanghai Enzyme Research Biotechnology Co., Ltd. and the Center for Excellence in Molecular and Cell Science, Chinese Academy of Sciences, respectively. The cells were cultured in RPMI 1640 medium supplemented with 10% heat-inactivated fetal bovine serum (GIBCO) (v/v) at 37°C in an atmosphere containing 5% CO_2. SPF-grade chicken eggs were
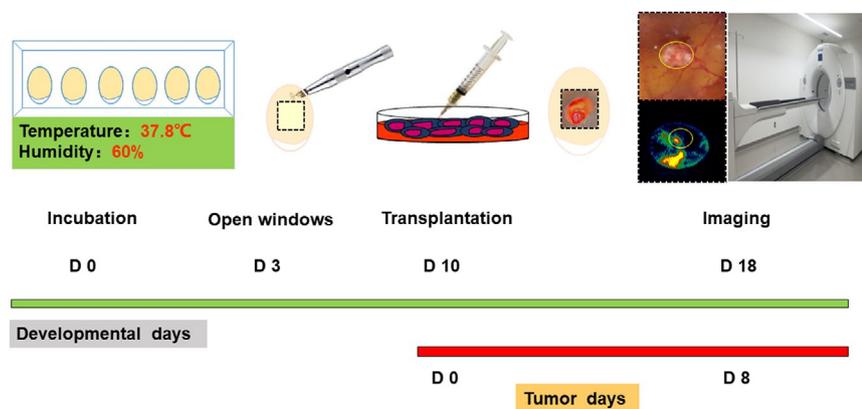

FIGURE 1 Schematic design of this study. The SPF-grade fertilized eggs were incubated in a constant temperature incubator for 3 days, and the windows were opened. The tumor cells were then inoculated in chicken chorioallantoic membrane (CAM) on Day 10 of incubation. The radioactive molecular probe was injected intravenously and micro positron emission tomography (PET) imaging was performed on Day 18 of incubation.

purchased from Beijing Boehringer Ingelhanwiton Biotechnology Co., Ltd. Female Balb/c nude mice 3–4 weeks old were purchased from Changzhou Cavens Laboratory Animal Co., Ltd.

2.4 | Cellular immunofluorescence

Bcap37 cells and MDA-MB-231 cells were cultured in 24 cell plates with a density of 1×10^5 cells/well until the cells converged to 75%–85% for immunofluorescence staining. After being washed with PBS for three times, the diluted primary antibody was added to the cells and incubated at 37°C for 2 h. Following this, the primary antibody was removed, and the cells were washed with PBS three times again. Then, the fluorescent secondary antibody was added and incubated at 37°C for 1 h. After being washed with PBS for three times, the tablet was sealed with DAPI, and the expression of the protein was observed under a fluorescence microscope.

2.5 | In vitro cellular uptake

Bcap37 cells and MDA-MB-231 cells were seeded in 24-well plates at a density of 1×10^5 cells/well and incubated overnight. After being washed with PBS for three times, ^{68}Ga-MZHER (37 KBq) was added to each well and incubated at 37°C. At 30 min and 90 min, respectively, the medium was replaced and washed three times with PBS. The cells were collected to determine the radioactivity in a γ-counter. The cell uptake value was normalized with the total radioactivity count, and the expression value was expressed as % AD/10^5 cells.

2.6 | Western blotting analysis

Bcap37 and MDA-MB-231 tumor cells were cultured to the logarithmic growth stage. After lysing using RIPA lysis buffer with 1 mM PMSF, the expression of HER2 and Ki67 in the tumor cells was determined following the kit protocols. After exposure and imaging, the protein bands were quantitatively analyzed using ImageJ software. Quantification analysis of Western gel was performed according to the literature.[18]

2.7 | Preparation of chicken CAM tumor model

The chicken CAM tumor models were established according to the previously reported methods.[17] Briefly, an incision was made on the eggshell surface to expose it on the third day of chicken embryo incubation. Bcap37 and MDA-MB-231 cells were routinely cultured in a constant temperature incubator at 37°C. On the seventh day of "opening the window," a 50-μL Matrigel mixture containing 5×10^6 tumor cells was inoculated into the chicken embryo CAM. After transparent sealing, the eggs were placed in the incubator for incubation. The tumor growth was monitored using a stereomicroscope at regular intervals.

2.8 | Preparation of mouse-bearing tumor

Approximately 5×10^6 tumor cells suspended in 0.2 mL PBS were subcutaneously implanted in the right front flank of female Balb/c nude mice. After tumor size reached 100–300 mm³, the animals were used for the following experiments.

2.9 | Micro PET imaging

Under the isoflurane anesthesia, the chicken CAM tumor models or mice-bearing tumors were placed at the center of the field of view of the micro PET scanner (Siemens Inc.) and injected with ^{68}Ga-MZHER (0.2 mL, 3.7 MBq) via CAM or the lateral tail vein, respectively. Static scanning with 10 min was performed at 30 and 90 min postinjection. The quantification analysis of PET images was performed using the same method as previously reported.[17,18]

2.10 | Biodistribution studies

After PET imaging, the chicken CAM and mice were killed, and the major organs were dissected and weighed. The radioactivity in the organs was determined using a γ-counter, and the corresponding uptake values were expressed as a percentage of the injected radioactive dose per gram of tissue (% ID/g).

2.11 | Histopathology

After PET imaging, the chicken embryo and mouse-human breast cancer graft specimens were taken and fixed, and the expressions of Ki67 and HER2 in each tumor sample were determined according to the literature.[13,19]

2.12 | Statistical analysis

Statistical analyses were performed using GraphPad Prism. Data were analyzed using the unpaired, two-tailed Student t-test. Differences at the 95% confidence level ($p < 0.05$) were considered to be statistically significant.

3 | RESULTS

3.1 | Immunofluorescence staining

Immunofluorescence staining showed that Ki67 was expressed in both Bcap37 and MDA-MB-231 cells at a close level ($p < 0.01$). HER2 expression level in Bcap37 tumor cells was significantly higher than those in MDA-MB-231 tumor cells (Figure 2A–C).

3.2 | In vitro analysis

The uptake value of Bcap37 cells was $2.85 \pm 0.12\%$ AD/10^5 cells at 30 min and increased to $3.77 \pm 0.19\%$ AD/10^5 cells at 90 min incubation, whereas the corresponding uptake value of MDA-MB-231 cells was $1.15 \pm 0.12\%$ AD/10^5 cells and $1.15 \pm 0.07\%$ AD/10^5 cells at 30 and 90 min postinjection, respectively ($p < 0.01$) (Figure 2D).

3.3 | Western blotting analysis

Meanwhile, the results of Western blotting analysis are presented in Figure 2E,F. It showed that HER2 was abundantly expressed in Bcap37 tumor cells but was significantly lower in MDA-MB-231 tumor cells.

3.4 | Animal models

Chicken embryo human breast cancer Bcap37 and MDA-MB-231 grew to 80–100 mm^3 after 8 days. The overall tumorigenic rates (number of tumorigenic chicken embryos/number of hatching chicken embryos) were $90.28 \pm 4.19\%$ for chicken embryo human breast cancer Bcap37 and $80.56 \pm 6.94\%$ for chicken embryo human breast cancer MDA-MB-231, respectively. To verify the reliability of the chicken embryo model, a mouse model was

established; the transplanted tumors in mice reached a volume of 200 mm^3 after 4 weeks. The total rates of tumor formation in mice were $86.75 \pm 1.97\%$ for the Bcap37 tumor and $68.28 \pm 1.67\%$ for the MDA-MB-231 tumor.

3.5 | In vivo micro PET imaging

Micro PET images showed that the radiotracer was rapidly distributed throughout the body and mainly concentrated in the heart, kidney, bladder, and other organs of both models (Figure 3A). The kidney is the main radioactive concentrated organ, which indicates that ^{68}Ga-MZHER is excreted primarily through the kidneys. At 30 min postinjection, the tumor uptake value of chicken CAM Bcap37 tumor was $5.36 \pm 0.26\%$ ID/g and increased to $5.86 \pm 0.29\%$ ID/g at 90 min postinjection (Figure 3B). The uptake value of muscle was $0.43 \pm 0.11\%$ ID/g and $0.26 \pm 0.09\%$ ID/g at 30 and 90 min postinjection. In contrast, the uptake value of chicken CAM MDA-MB-231 tumors was $1.57 \pm 0.15\%$ ID/g at 30 min postinjection and $1.32 \pm 0.16\%$ ID/g at 90 min postinjection. The uptake value of muscle was $0.41 \pm 0.10\%$ ID/g and $0.30 \pm 0.08\%$ ID/g at 30 and 90 min, respectively ($p < 0.01$).

The PET images of mice bearing breast cancer are shown in Figure 3C. The tumor uptake value of Bcap37 at 30 min was $5.26 \pm 0.43\%$ ID/g, and the muscle uptake value was $0.53 \pm 0.12\%$ ID/g (Figure 3D). At 90 min, the uptake values of Bcap37 tumor
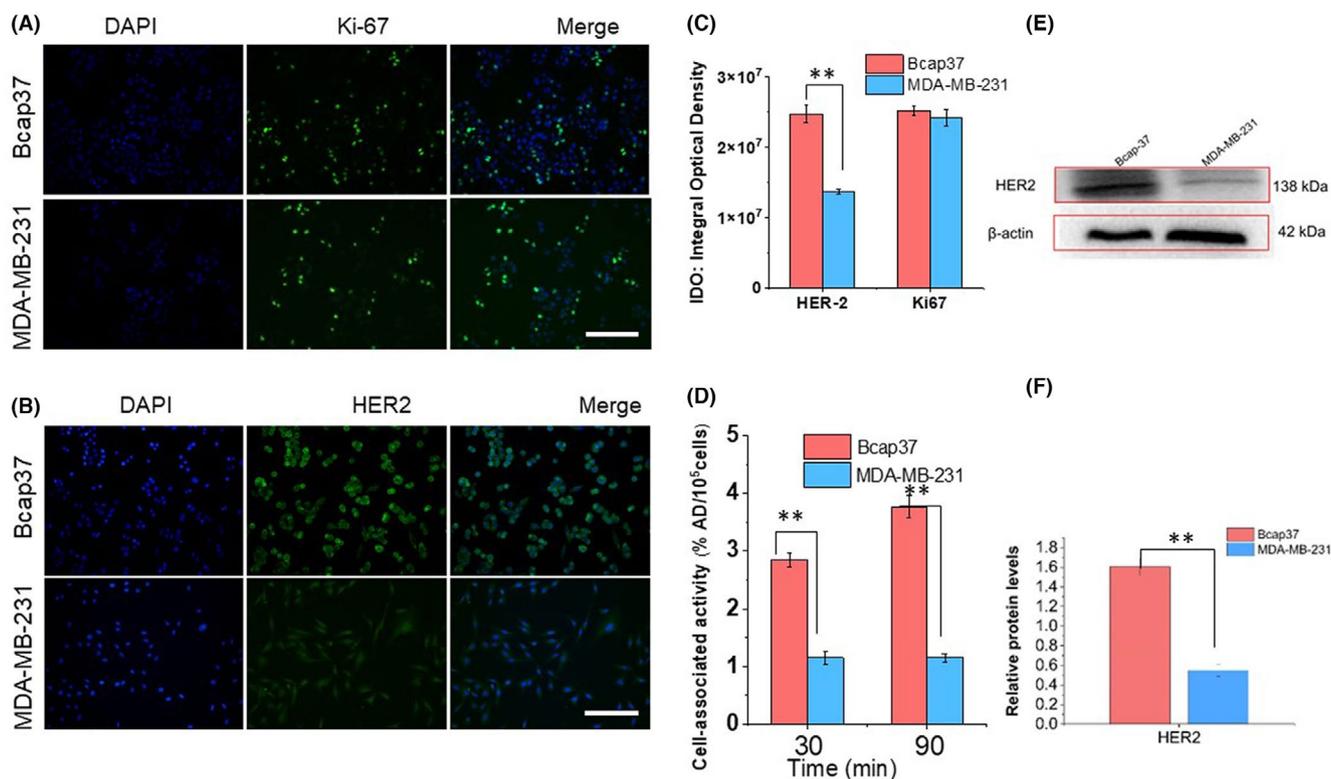

FIGURE 2 Immunofluorescence of Bcap37 and MDA-MB-231 tumor cells (A,B). Analysis of the expression of HER2 and Ki67 in tumor cells (C). Uptake value of the tumor cells after incubation with ^{68}Ga-MZHER (D). Western blots and analysis of HER2 in two tumor cells (E,F).
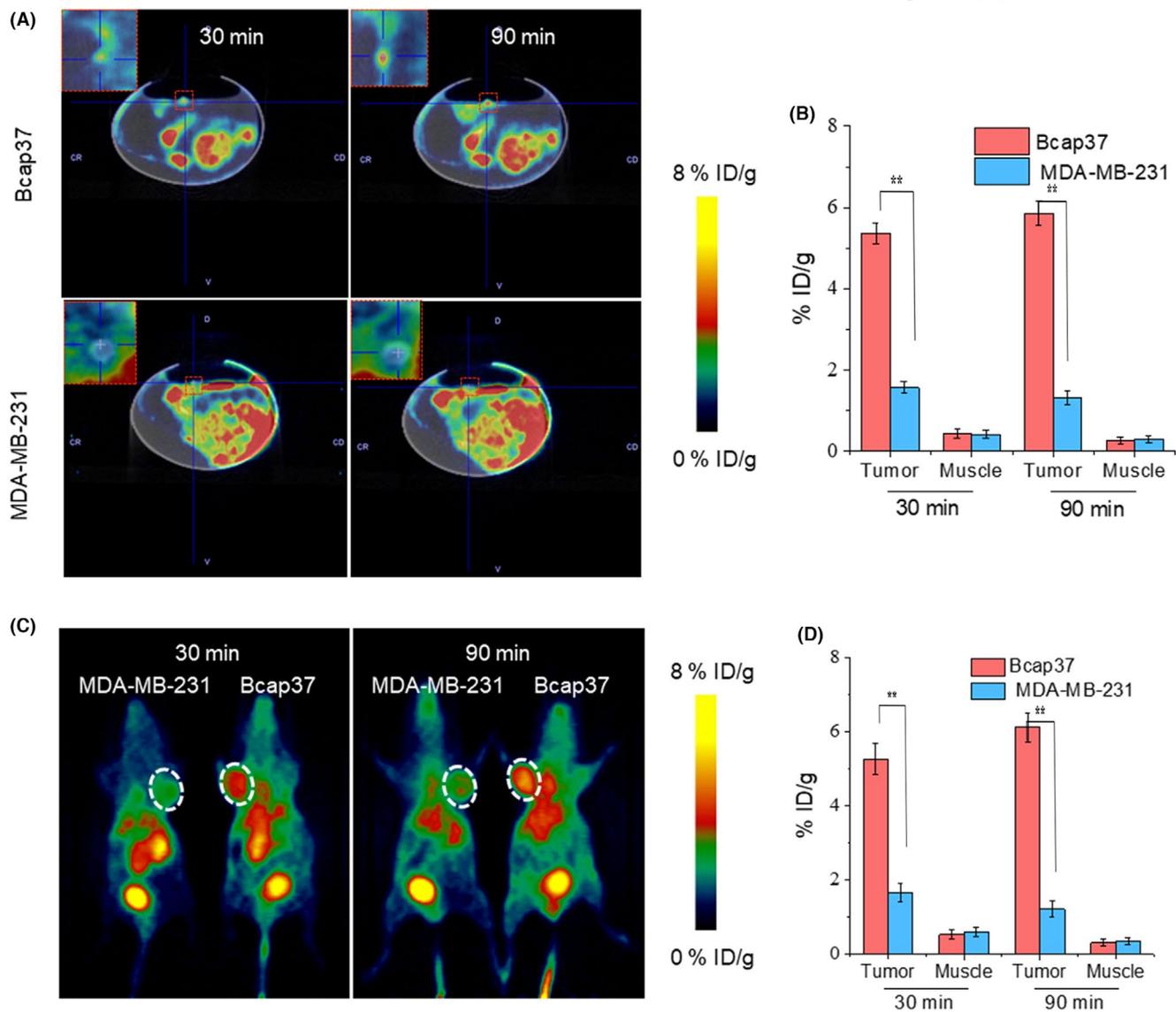
FIGURE 3 Positron emission tomography (PET) images of the chicken chorioallantoic membrane (CAM) (A) and mouse tumor models (C) after injection of ^{68}Ga-MZEHR. PET quantification analysis for uptakes of tumor and muscles in the chicken CAM (B) and mouse tumor models (D).

and muscle were $6.12 \pm 0.39\%$ ID/g and $0.32 \pm 0.1\%$ ID/g, respectively. At the same time, the uptake value of MDA-MB-231 tumors in mice at 30 min was $1.67 \pm 0.25\%$ ID/g, and the muscle uptake value was $0.61 \pm 0.13\%$ ID/g (Figure 3D). At 90 min, the uptake values of the MDA-MB-231 tumor were $1.22 \pm 0.21\%$ ID/g ($p < 0.01$).

3.6 | H&E and immunohistochemistry

In both chicken CAM and mouse models, hematoxylin and eosin (H&E) staining showed an increased nucleus-to-plasma ratio, dense arrangement of tumor cells, and visible mitotic phase (Figure 4). Immunohistochemical staining showed that both Bcap37 and MDA-MB-231 expressed Ki67, indicating that tumor

cells were proliferating. HER2 staining showed positive expression of Bcap37 cells, mainly in membranes, and low HER2 expression in MDA-MB-231 cells, which were consistent with micro PET imaging results.

3.7 | Ex vivo biological distribution

After micro PET imaging, both chicken embryo and mice were executed, and the biological distribution results are summarized in Tables 1 and 2. The uptake values of ^{68}Ga-MZHER by Bcap37 and MDA-MB-231 transplanted tumors in the chicken embryo were $5.98 \pm 0.31\%$ ID/g and $1.20 \pm 0.12\%$ ID/g at 90 min postinjection, respectively. At the same time point, the uptake values of Bcap37 and MDA-MB-231 xenografted mouse models were $4.38 \pm 0.13\%$
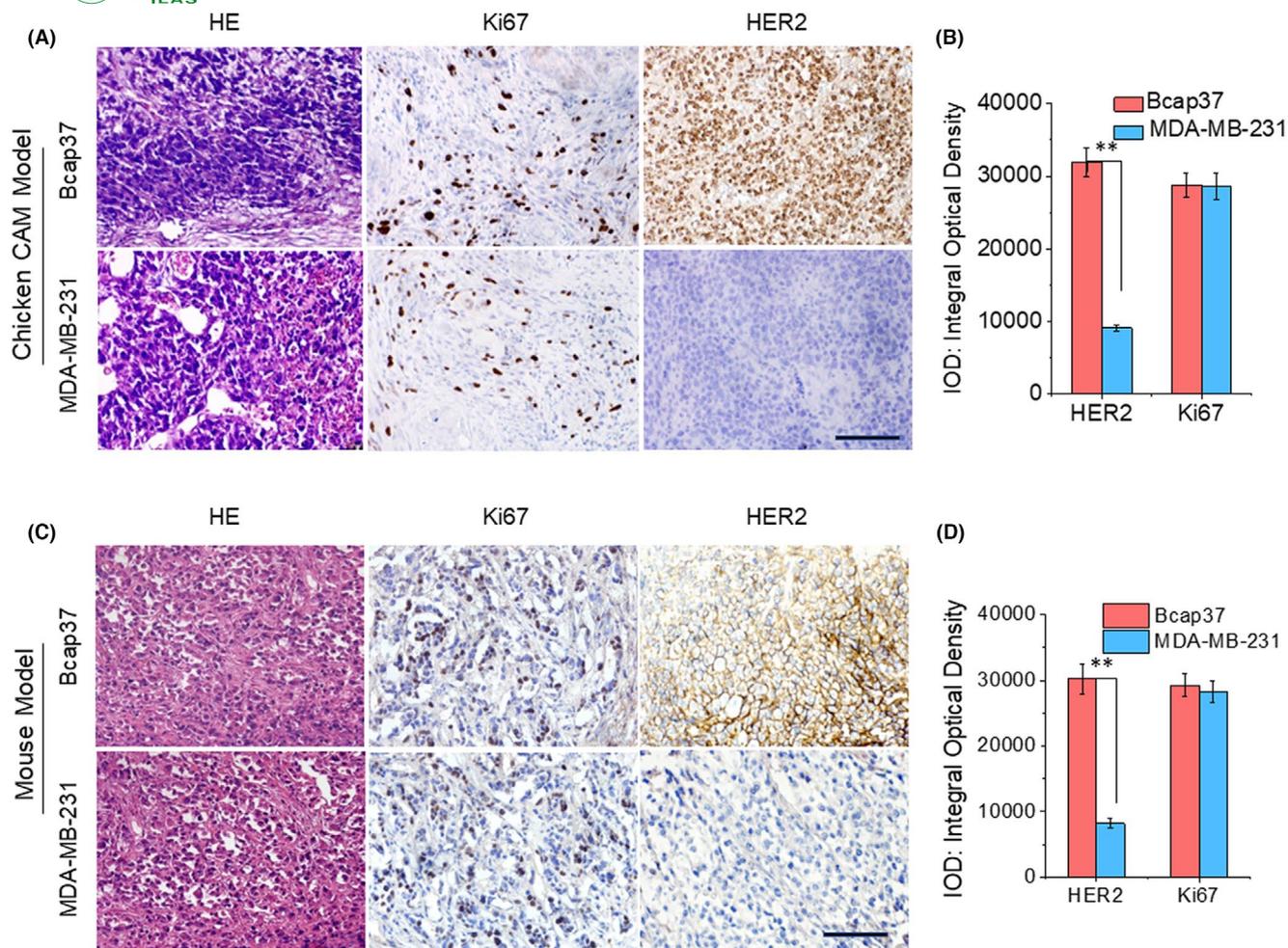
FIGURE 4 Hematoxylin and eosin (H&E) and immunohistochemical results (Ki67, HER2) (A,C). Analysis of tumor sections from ^{68}Ga-MZHER-administrated MDA-MB-231 and Bcap37 tumors inoculated in chicken embryos and mice and the corresponding data analysis (B,D).

TABLE 1 Biological distribution of ^{68}Ga-MZHER in chicken embryo graft tumor % ID/g ($n=4$).

Organs (% ID/g)	Bcap37	MDA-MB-231
Blood	0.80±0.12	1.32±0.14
Brain	0.52±0.11	0.35±0.07
Heart	0.88±0.11	0.90±0.19
Liver	1.77±0.14	1.39±0.14
Lung	1.21±0.11	1.36±0.10
Kidney	101.31±11.89	123.31±8.59
Stomach	1.08±0.21	1.03±0.15
Intestinal	1.14±0.20	1.27±0.13
Muscle	0.24±0.08	0.24±0.10
Bone	1.29±0.07	1 47±0.12
Tumor	5.98±0.31	1.20±0.12

TABLE 2 Biological distribution of ^{68}Ga-MZHER in mouse tumor grafts % ID/g ($n=4$).

Organs (% ID/g)	Bcap37	MDA-MB-231
Blood	0.98±0.12	1.29±0.10
Brain	0.50±0.13	0.34±0.04
Heart	1.09±0.11	0.94±0.16
Liver	1.57±0.26	1.31±0.20
Spleen	1.36±0.23	1.46±0.10
Lung	1.11±0.09	1.31±0.11
Kidney	110.81±10.13	126.31±13.65
Stomach	1.08±0.15	1.00±0.22
Intestinal	1.21±0.21	1.27±0.12
Muscle	0.24±0.06	0.25±0.06
Pancreas	0.68±0.06	0.76±0.06
Bone	1.32±0.19	1.69±0.26
Tumor	6.38±0.13	1.38±0.13

ID/g and 1.08±0.03% ID/g, respectively. Lower levels of radioactivity were observed in the blood and most other organs. Among the normal tissues, high activity accumulation was also found in the kidney for all models. The uptakes in the kidney were 101.31±11.89% ID/g and 123.31±8.59% ID/g at 90 min postinjection in the chick

CAM-bearing Bcap37 and MDA-MB-231 tumors, respectively. These values were similar to those in mice bearing the counterpart tumors (110.81±10.13% ID/g and 126.31±13.65% ID/g, respectively).

4 | DISCUSSION

A suitable and effective experimental model reflecting the complexities of pathogenesis pathways or genomic variations in tumors was needed for precision medicine in oncology. The chick CAM model seemed to be a favorable platform for the studies of human cancer, which enables the transplantation of tumors using cancer cell lines or patient-derived xenografts (PDX).[20–22] In general, the extended time to acquire xenografts in CAM models for in vivo studies was nearly 2–10 days. In contrast, the duration to establish the graft in the murine always could range from 15 days to 6 months depending on the sources of transplanted tumors (cancer cell lines or PDX) and the immunodeficiency backgrounds of the mouse strains. Thus, the turnover time to evaluate the drug efficacies is only 2 weeks in chick CAM models compared to 3–6 months in mouse models. Moreover, the chick CAM model is more cost-effective than the immunodeficient mice, as no additional forage was required. It implied that the chick CAM model is beneficial for drug development and individualized treatment in the clinic.[23–26]

Recently published literature revealed that CAM tumor models have been used for PET imaging with ^{18}F-labeled small molecules (^{18}F-FDG, ^{18}F-siPSMA-14) and ^{89}Zr-labeled human serum albumin.[17,27,28] However, few CAM models have been employed for noninvasive assessment of the biodistribution and accumulation of radiolabeled peptides. In this study, we investigated the potential of the chicken CAM model as an alternative to animal models for evaluating the in vivo imaging properties of radiolabeled peptides.

In vitro Western blotting assay and immunofluorescence confirmed that the HER2 levels of the two human breast tumor cells were significantly different. Further, in vitro cell uptake study showed that the uptakes of the HER2-specific probe in Bcap37 tumor cells with high levels of HER2 were significantly higher than those in MDA-MB-231 tumor cells with low levels of HER2. Thus, the two human breast cancer cells were transplanted into the chicken CAM and mice, respectively, for the following experiments. Ex vivo immunohistochemistry assay revealed that the xenograft in the chicken CAM owns the same characteristics as those in the mouse. It was found that the HER2 levels in Bcap37 xenograft were nearly two to three times those of MDA-MB-231 xenograft at the chicken CAM models, which was consistent with the outcomes in mouse xenograft models. Similar to the findings of ex vivo immunohistochemistry, in vivo PET imaging showed that uptake values of ^{68}Ga-MZHER in HER2-positive Bcap37 tumors were also about two to three times higher than those in HER2-negative MDA-MB-231 tumors both in CAM and mouse xenograft models. Further biodistribution studies confirmed that the metabolism routes of the peptide were agreed with the counterparts in the mouse xenograft models. It implied that the CAM model could be used for evaluating the in vivo performance of radiolabeled peptides.

Despite these, there also existed limitations in the chick CAM models. Due to physiological and tumor growth time differences, the weight and volumes of the xenograft tumor in the chicken CAM models were nearly onefold lower than those in the mouse model. Administration of a large cell number into the chicken CAM might obtain a large tumor and overcome the shortcoming. Meanwhile, according to the published literature, the chicken CAM with metastasis tumors could be obtained by directly injecting the tumor cells into the allantoic vein. The application of PET imaging in the CAM models with metastasis tumors will be evaluated in future works.[29]

In general, the affordable CAM model is suitable for quickly determining the in vivo imaging properties of radiolabeled peptides targeting HER2 and other biomarkers in tumors. Besides, it may be beneficial for early monitoring of the therapeutic effect of targeted agents through PET imaging. Further experiments are ongoing.

DATA AVAILABILITY STATEMENT

The authors declare no competing financial interests or other associations that may pose a conflict of interest. Raw data were generated at Anhui Agricultural University and the Jiangsu Institute of Nuclear Medicine. The raw data supporting the conclusions of this article will be made available by the authors, without undue reservation. All data generated during this study are included in the published article.

ORCID

Jian Tu https://orcid.org/0000-0002-5964-5634

REFERENCES

1. Moradipoodeh B, Jamalan M, Zeinali M, Fereidoonnezhad M. Specific targeting of HER2-positive human breast carcinoma SK-BR-3 cells by amygdaline-ZHER2 affibody conjugate. *Mol Biol Rep.* 2020;47(9):7139-7151. doi:10.1007/s11033-020-05782-z

2. Harbeck N. Advances in targeting HER2-positive breast cancer. *Curr Opin Obstet Gynecol.* 2018;30(1):55-59. doi:10.1097/GCO.0000000000000431

3. Guo X, Zhu H, Zhou N, et al. Noninvasive detection of HER2 expression in gastric cancer by ^{64}Cu-NOTA-Trastuzumab in PDX mouse model and in patients. *Mol Pharm.* 2018;15(11):5174-5182. doi:10.1021/acs.molpharmaceut.8b00673

4. Pernas S, Tolaney SM. HER2-positive breast cancer: new therapeutic frontiers and overcoming resistance. *Ther Adv Med Oncol.* 2019;11:1758835919833519. doi:10.1177/1758835919833519

5. Arciero CA, Guo Y, Jiang R, et al. ER$^+$/HER2$^+$ breast cancer has different metastatic patterns and better survival than ER$^-$/HER2$^+$ breast cancer. *Clin Breast Cancer.* 2019;19(4):236-245. doi:10.1016/j.clbc.2019.02.001

6. Liu Y, Wang L, Pan D, et al. PET evaluation of light-induced modulation of microglial activation and GLP-1R expression in depressive rats. *Transl Psychiatry.* 2021;11(1):26. doi:10.1038/s41398-020-01155-z

7. Zlatopolskiy BD, Zischler J, Schäfer D, et al. Discovery of 7-[^{18}F]Fluorotryptophan as a novel positron emission tomography (PET) probe for the visualization of tryptophan metabolism in vivo. *J Med Chem.* 2018;61(1):189-206. doi:10.1021/acs.jmedchem.7b01245

8. Alhuseinalkhudhur A, Lindman H, Liss P, et al. Human epidermal growth factor receptor 2-targeting [^{68}Ga]Ga-ABY-025 PET/CT predicts early metabolic response in metastatic breast cancer. *J Nucl Med.* 2023;64(9):1364-1370. doi:10.2967/jnumed.122.265364

9. Han J, Chen Y, Zhao Y, et al. Pre-clinical study of the [^{18}F]AIF-labeled HER2 affibody for non-invasive HER2 detection in gastric cancer. *Front Med (Lausanne).* 2022;9:803005. doi:10.3389/fmed.2022.803005

10. Miladinova D. Molecular imaging of HER2 receptor: targeting HER2 for imaging and therapy in nuclear medicine. *Front Mol Biosci.* 2023;10:1144817. doi:10.3389/fmolb.2023.1144817

11. Zhou N, Liu C, Guo X, et al. Impact of ^{68}Ga-NOTA-MAL-MZHER2 PET imaging in advanced gastric cancer patients and therapeutic response monitoring. *Eur J Nucl Med Mol Imaging.* 2021;48(1):161-175. doi:10.1007/s00259-020-04898-5

12. Miao H, Sun Y, Jin Y, Hu X, Song S, Zhang J. Application of a novel ^{68}Ga-HER2 affibody PET/CT imaging in breast cancer patients. *Front Oncol.* 2022;12:894767. doi:10.3389/fonc.2022.894767

13. Xu Y, Wang L, Pan D, et al. PET imaging of a ^{68}Ga labeled modified HER2 affibody in breast cancers: from xenografts to patients. *Br J Radiol.* 2019;92(1104):20190425. doi:10.1259/bjr.20190425

14. Chu P-Y, Koh AP-F, Antony J, Huang RY-J. Applications of the Chick Chorioallantoic membrane as an alternative model for cancer studies. *Cells Tissues Organs.* 2022;211(2):222-237. doi:10.1159/000513039

15. Pinto MT, Ribeiro AS, Conde I, Carvalho R, Paredes J. The chick chorioallantoic membrane model: a new in vivo tool to evaluate breast cancer stem cell activity. *Int J Mol Sci.* 2020;22(1):334. doi:10.3390/ijms22010334

16. Pomraenke M, Bolney R, Winkens T, et al. A novel breast cancer xenograft model using the ostrich Chorioallantoic membrane-a proof of concept. *Vet Sci.* 2023;10(5):349. doi:10.3390/vetsci10050349

17. Hilbrig C, Löffler J, Fischer G, et al. Evaluation of the EPR effect in the CAM-model by molecular imaging with MRI and PET using ^{89}Zr-labeled HAS. *Cancers (Basel).* 2023;15(4):1126. doi:10.3390/cancers15041126

18. Xu Y, Bai Z, Huang Q, et al. PET of HER2 expression with a novel ^{18}FAl labeled affibody. *J Cancer.* 2017;8(7):1170-1178. doi:10.7150/jca.18070

19. Xu Y, Wang L, Pan D, et al. Synthesis of a novel ^{89}Zr-labeled HER2 affibody and its application study in tumor PET imaging. *EJNMMI Res.* 2020;10(1):58. doi:10.1186/s13550-020-00649-7

20. Veinotte CJ, Dellaire G, Berman JN. Hooking the big one: the potential of zebrafish xenotransplantation to reform cancer drug screening in the genomic era. *Dis Model Mech.* 2014;7(7):745-754. doi:10.1242/dmm.015784

21. Jung J, Seol HS, Chang S. The generation and application of patient-derived xenograft model for cancer research. *Cancer Res Treat.* 2018;50(1):1-10. doi:10.4143/crt.2017.307

22. Ribatti D. The chick embryo chorioallantoic membrane as a model for tumor biology. *Exp Cell Res.* 2014;328(2):314-324. doi:10.1016/j.yexcr.2014.06.010

23. Haller S, Ametamey SM, Schibli R, Müller C. Investigation of the chick embryo as a potential alternative to the mouse for evaluation of radiopharmaceuticals. *Nucl Med Biol.* 2015;42(3):226-233. doi:10.1016/j.nucmedbio.2014.10.010

24. Chen L, Wang S, Feng Y, et al. Utilisation of Chick embryo Chorioallantoic membrane as a model platform for imaging-navigated biomedical research. *Cell.* 2021;10(2):463. doi:10.3390/cells10020463

25. Sajjad H, Imtiaz S, Noor T, Siddiqui YH, Sajjad A, Zia M. Cancer models in preclinical research: a chronicle review of advancement in effective cancer research. *Animal Model Exp Med.* 2021;4(2):87-103. doi:10.1002/ame2.12165

26. Monzavi SM, Muhammadnejad A, Behfar M, Khorsand AA, Muhammadnejad S, Kajbafzadeh AM. Spontaneous xenogeneic GvHD in Wilms' tumor patient-derived xenograft models and potential solutions. *Animal Model Exp Med.* 2022;5(4):389-396. doi:10.1002/ame2.1225427

27. Warnock G, Turtoi A, Blomme A, et al. In vivo PET/CT in a human glioblastoma chicken chorioallantoic membrane model: a new tool for oncology and radiotracer development. *J Nucl Med.* 2013;54(10):1782-1788. doi:10.2967/jnumed.112.117150

28. Löffler J, Hamp C, Scheidhauer E, et al. Comparison of quantification of target-specific accumulation of [^{18}F]F-siPSMA-14 in the HET-CAM model and in mice using PET/MRI. *Cancers (Basel).* 2021;13(16):4007. doi:10.3390/cancers13164007

29. Patten LW, Blatchford P, Strand M, Kaizer AM. Assessing the performance of different outcomes for tumor growth studies with animal models. *Animal Model Exp Med.* 2022;5(3):248-257. doi:10.1002/ame2.12250